Journal of Optoelectronics and Advanced Materials Vol. 5, No. 3, September 2003, p. 627 - 634

STRUCTURAL FEATURES OF FLUORIDE-ION TRANSPORT IN $Pb_{0.67}Cd_{0.33}F_2$ SINGLE CRYSTALS

V. Trnovcová[a,b*], P. P. Fedorov[c], M. Ožvoldová[a], I. I. Buchinskaya[c], E. A. Zhurova[c]

[a]Faculty of Materials Science and Technology, Slovak University of Technology, SK- 91724 Trnava, Slovakia
[b]Institute of Physics, Slovak Academy of Sciences, SK-84228 Bratislava, Slovakia
[c]Shubnikov Institute of Crystallography, Russian Academy of Sciences, Moscow 117333, Russia

Using the X-ray single crystal diffraction technique, the crystal structure of the $Pb_{0.67}Cd_{0.33}F_2$ single crystal was studied. This fluorite-structured crystal (space group *Fm*3*m*, *a* = 0.57575(4) nm) has the highest ionic conductivity of the $Pb_{1-x}Cd_xF_2$ solid solutions. The statistical displacement of cations achieves 0.05 nm, and the deficiency of fluoride ions in lattice positions is equal to 25±2 %. From the measured temperature dependence of the ionic conductivity, $\sigma T = (1.2\pm0.3) \times 10^7 \exp(-0.359\pm0.007/kT)$, we have calculated the temperature dependence of the hopping frequency of fluoride ions. Upon doping with 1m/o LiF and with 1 or 3 m/o NaF, the ionic conductivity decreases. For doped crystals, the equation $\sigma T = (1.4\pm0.2)\cdot10^7 \exp(-0.389\pm0.005/kT)$ is valid.

(Received July 15, 2003; accepted July 31, 2003)

Keywords: Fast ionic conductivity, Fluoride ion hopping frequency, Phase diagram, Defect concentration, Single crystal, Lead fluoride, Cadmium fluoride

1. Introduction

In the PbF_2-CdF_2 system, the highest ionic conductivity ($\sigma = 8\cdot10^{-5}$ S cm^{-1} at 300 K) and the lowest conduction activation energy (E = 0.38 eV) were found at ~35 mole % CdF_2 [1]. This conductivity, measured on pressed pellets, is close to those of the best fluoride ion conductors [2,3]. The composition of the solid solution corresponds approximately to the minimum of the melting curves of the PbF_2-CdF_2 system [4,5].

To explain the high ionic conductivity, which corresponds to the minimum of the melting curves of the PbF_2-CdF_2 system, we needed data about its crystal structure of this solid solution. Precise data about the crystal structure of fluoride-ion conductors are usually obtained by neutron diffraction techniques. However, such studies are impossible for $Pb_{1-x}Cd_xF_2$ solid solutions because of the high value of neutron capture cross-section of Cd nuclei.

The aim of this work was
- to refine the PbF_2-CdF_2 phase diagram and the position of the minimum of the melting curves;
- to determine the precise crystal structure for the single crystal corresponding to the minimum of the melting curves;
- to measure the ionic conductivity of this crystal;
- to determine the influence of a doping with monovalent cations on the ionic conductivity.

2. Experimental

Cadmium and lead fluorides of 99.9 % purity were used as starting reagents. They were remelted under fluorinating atmosphere of Teflon pyrolysis products. Cadmium fluoride was additionally refined by a directional crystallization.

* Corresponding author: fyzitrno@mtf.stuba.sk

The phase diagram was studied using the differential thermal analysis (DTA) and X-ray powder diffraction analysis (XRPDA). The DTA was performed under He, in graphite crucibles. The mass of the sample was 1 g, the cooling and heating rates were equal to 10-30 K/min. The temperatures of liquidus and solidus curves were determined from the onset of corresponding peaks on cooling and heating curves, respectively. The melting temperatures are 825±5 °C or 1075±5 °C for PbF_2 and CdF_2 crystals, respectively. These temperatures agree well with literature data (820 °C for PbF_2 [4,6], and 1075 °C for CdF_2 [4]). We have studied the effect of the cooling rate on the solidification temperature of both components. For a cooling rate lower than 100 K/min, a supercooling of the melt did not occur.

To check the possible ordering or decomposition of the PbF_2 - CdF_2 solid solutions, we have performed a low-temperature solid-state annealing of samples. Carefully ground mixtures of the components were packed into Cu capillaries and put into a Cu bomb (with Teflon and $BaF_2 \cdot HF$ as fluorinating agents). Then, the bomb was welded. The time and temperatures of annealing were as follows: 400 h, and 600 °C, 650 °C or 680 °C. After annealing, the bomb was quenched into water.

The XRPDA was performed using diffractometers AVF-202E, Toshiba (Japan) or HZG-4 (Germany), with CuK_α radiation. Silicon was used as an internal standard, when determining the lattice parameter.

The single crystals of $Cd_{0.33}Pb_{0.67}F_2$ and PbF_2 were grown by the Bridgman technique, in an evacuated chamber, under a fluorinating atmosphere of Teflon-pyrolysis products, using graphite crucibles. The rate of lowering of the crucible was equal to 3.5 mm/h. The cooling rate to room temperature was equal to 100 °C/h. We have prepared both "pure" $Cd_{0.33}Pb_{0.67}F_2$ crystals and the crystals doped with monovalent cations (1 m/o LiF or NaF and 3 m/o NaF).

The XRPDA data were obtained from a spherical sample, 0.185(5) mm in diameter, using a CAD-4 Enraf Nonius diffractometer (with AgK_α radiation) and a secondary graphite monochromator.

The ionic conductivity was measured using a SI 1260 Impedance/gain analyzer, Schlumberger-Solartron, at frequencies from 1 Hz to 10 MHz, over the temperature range from 20 °C to 440 °C. Silver electrodes (Leitsilber) were painted on parallel surfaces of samples. Before measurements, the samples with applied contacts were annealed at 400 °C for 1 h, under dry Ar. The measurements were performed under dry Ar, both with a heating rate of 2 K/min and under isothermal conditions, after 1 hour's annealing at the given temperature. The bulk conductivity (σ_{dc}) was calculated using the impedance analysis. The static relative permittivity (ε_s) was determined using the modular analysis.

We suppose that silver electrodes do not interact with samples because 1) the X-ray analysis of the samples after electrical measurements shows only lines of a metallic silver, 2) the time of annealing does not influence the result of a subsequent electrical measurement, and 3) repeated electrical measurements (up to 440 °C) give the same results.

3. Results

Fig. 1 shows a refined phase diagram of the PbF_2-CdF_2 system. The existence of a continuous range of solid solutions between PbF_2 and CdF_2 was confirmed over the temperature range from 500 °C to 690 °C. The XRPDA patterns of annealed and quenched samples show that the lattice parameter of the solid solutions decreases linearly with an increasing molar fraction of the CdF_2 component (from the value of 5.940 Å for the PbF_2 component to that of 5.388 Å for the CdF_2 component). No additional superstructure reflections and no split of parent structure reflections (they indicate an ordering of the solid solution) have been observed. Within the studied temperature range, no decomposition of the solid solutions was observed.

Our data reveal that the coordinates of the minimum, where the solidus and liquidus lines coincide and have a common horizontal tangent, are equal to 33±1 mole % of CdF_2 and 750±5 °C. This result is close to those obtained in [4] and is in agreement with data which were obtained using directional crystallization [5]. The composition of the minimum point, $Pb_{0.67}Cd_{0.33}F_2$, is the same as the stoichiometric composition Pb_2MF_6.

The liquidus and solidus curves in the vicinity ($0.08 < x < 0.6$) of the minimum can be described, with the accuracy of ±7°C, by equations

$$T_L - T_o = 810 (x - x_o)^2 \quad (1)$$

$$T_S - T_o = 487 (x - x_o)^2 \quad (2)$$

where T_L and T_S are the liquidus and solidus temperatures, respectively, and x is the molar fraction of CdF_2, $T_o = 750$ °C , $x_o = 0.33$.

A congruent melting behavior of the $Pb_{0.67}Cd_{0.33}F_2$ solid solution made it possible to grow single crystals without a cell substructure, with a homogeneous distribution of components [7]. Mechanical and optical properties of prepared $Pb_{0.67}Cd_{0.33}F_2$ crystals are described in [7].

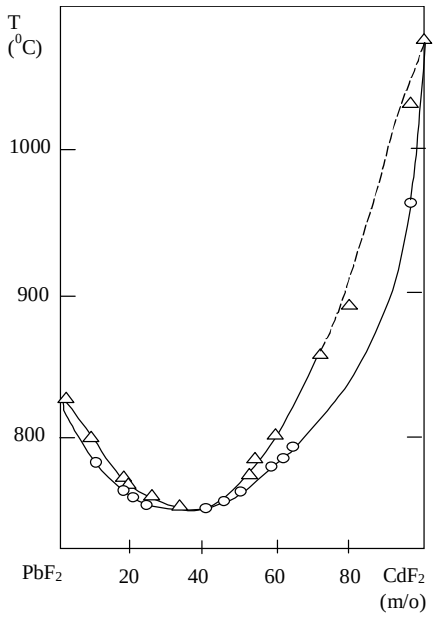

Fig. 1. Phase diagram of the PbF_2–CdF_2 system (DTA data).

In the X-ray single crystal diffraction data, 480 independent reflections were detected. After rejection of some weak reflections by profile considerations and averaging of symmetrically equivalent reflections (R factor is equal to R_{int}= 3.3 %), 64 independent reflections were obtained within the range of $\sin\theta/\lambda$, from 0 to 10.4 nm^{-1}. The space group of the crystal symmetry is *Fm*3*m*, the unit-cell parameter, *a*, is equal to 0.57676(4) nm. Intensities of the reflections were corrected for the Lorentz factor, polarization, and absorption. The refinement of the crystal structure was performed until R = 1.2 %, R_w = 1.08 %, and S = 1.69. The electron synthesis pattern is presented in Fig. 2. In the subtracted model used, we have taken into account that the *4a* cationic positions are statistically occupied by Cd and Pb atoms and that the *8c* fluorine positions are occupied by 75 % (q_F=0.75(2)). Close to the *4b* positions with coordinates (1/2, 1/2, 1/2), there are several peaks of the electron density that can be attributed to additional (interstitial) positions of the fluorine ions. The total number of fluorine ions in these positions must be equal to the number of these ions lacking in the basic position. "Bridges" of a continuous electron density connect possible positions of these ions.

In Fig. 2, additional peaks of electron density can be observed near the origin of the coordinates. They may correspond to a splitting of the *4a* cationic positions. The peaks correspond to displacements of cations along the threefold and fourfold axes. Under the assumption that Cd cations are placed evenly in these displaced positions, calculations resulted in an essential refinement of the electron synthesis pattern.

In Fig. 3, the temperature dependence of the bulk ionic conductivity of the $Pb_{0.67}Cd_{0.33}F_2$ single crystal is presented and compared with that of the "pure" PbF_2 single crystal. It can be described by the equation

$$\sigma T = (1.2\pm0.3)\cdot10^7 \exp(-0.359\pm0.007/kT), \qquad (S\ K\ m^{-1}) \qquad (3)$$

The ionic conductivity at room temperature ($\sigma_{300} = 3.5\cdot10^{-2}$ S m^{-1}), is close to that of the best fluoride ion conductors [5,8].

Upon doping with NaF or LiF, the value of the ionic conductivity slightly decreases (Fig. 3). The temperature dependence of the ionic conductivity of all doped crystals can be described by the equation

$$\sigma T = (1.4\pm0.3)\cdot10^7 \exp(-0.389\pm0.005/kT), \qquad (S\ K\ m^{-1}) \qquad (4).$$

A decrease of the conductivity upon doping with monovalent cations results from an increase of the conduction activation enthalpy. The pre-exponential factor is not influenced by doping. Such a behavior is typical for disordered and glassy systems.

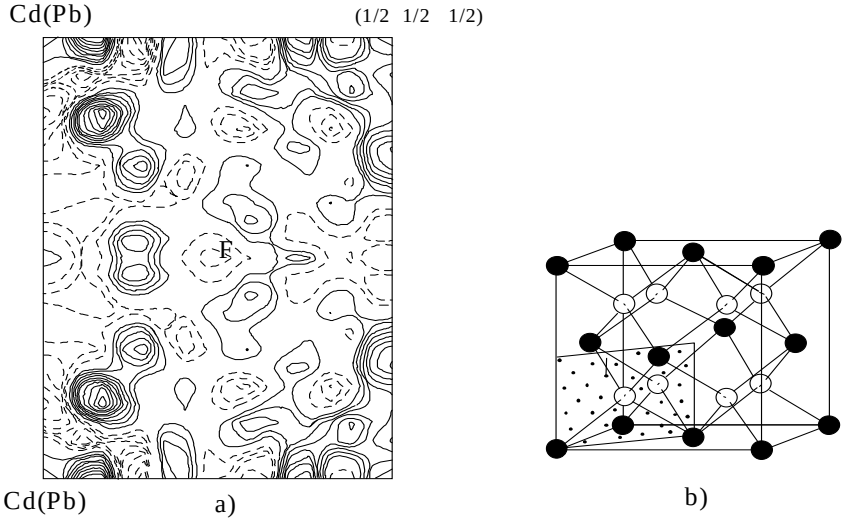

Fig. 2. Electron density difference map through the (101) plane (a), and the section position in the fluorite structure (b). The distance between isolines is equal to 10^2 e·nm^{-3}. Dashed lines correspond to negative contours, solid lines correspond to positive contours.

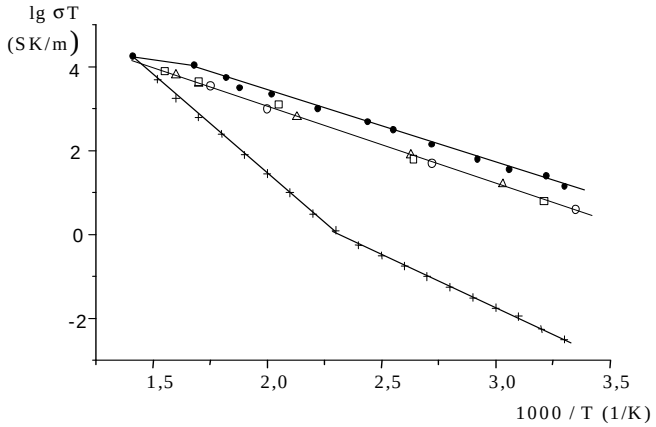

Fig. 3. Temperature dependence of the bulk ionic conductivity of fluorite-structured PbF_2 (+), $Pb_{0.67}Cd_{0.33}F_2$ (•), $Pb_{0.67}Cd_{0.33}F_2$:1 m/o LiF (Δ), $Pb_{0.67}Cd_{0.33}F_2$:1 m/o NaF (□), and $Pb_{0.67}Cd_{0.33}F_2$ (o) single crystals.

In the entire temperature range, the admittance diagrams of both "pure" and doped $Pb_{0.67}Cd_{0.33}F_2$ single crystal are shifted from the origin (Fig. 4). The value of this shift, $\Delta\sigma$, is rather independent of the temperature but it depends on the type and concentration of monovalent dopants. For "pure" crystals, $\Delta\sigma$ = 0.34(1) S m^{-1}. For crystals doped with 1 m/o LiF, $\Delta\sigma$ = 0.8(1) S m^{-1}. For crystals doped with 1 m/o NaF or 3 m/o NaF, the value of $\Delta\sigma$ is equal to 0.8(1) S m^{-1} and 0.5(1) S m^{-1}, respectively. This shift is connected with a frequency independent component of the conductivity. It was not observed in "pure" and doped PbF_2 crystals [9] but it was observed in the $Pb_{0.67}Cd_{0.33}F_2$-NaF composites [10]. The cause of this shift is not yet clear but it coincides with a presence of Cd-component in various materials [11].

The value of the static relative permittivity in both "pure" and doped $Pb_{0.67}Cd_{0.33}F_2$ single crystals is equal to 23(1).

4. Discussion

4.1. Splitting of cationic positions

The observation of additional cationic positions indicates some shift of cations from the *4a* positions along both the threefold and fourfold axes. This result correlates with data of EXAFS studies about a disorder in the $Pb_{1-x}Cd_xF_2$ solid solutions [12,13]. For the $Pb_{0.6}Cd_{0.4}F_2$ composition, a comparative analysis of the Fourier transformation of experimental data demonstrates that the Pb-F bond length is longer than the Cd-F one (2.471Å and 2.287 Å at 300 K, respectively) [12]. This fact can be easily explained when we take into account the significantly different sizes of the two isomorphous cations. The cation-anion, M^{2+}-F^-, distances in PbF_2 and CdF_2 (calculated as $a\sqrt{3}/4$, where a is the cell parameter) are equal to 2.572 Å and 2.333 Å, respectively. This is the largest difference (10 %) of ionic radii that still tolerates a formation of continuous series of fluorite-type solid solutions in the MF_2-$M'F_2$ systems. Therefore, the BaF_2-CdF_2 system exemplifies a formation of the ordered stoichiometric compound [4]. In the BaF_2-CaF_2 system, a total decomposition of the solid solutions takes place when the temperature is lowered [14]. Only limited solid solutions are formed in the peritectic-type PbF_2-CaF_2 phase diagram [15]. In the $Pb_{0.67}Cd_{0.33}F_2$ solid solution, the average M^{2+}-F^- distance is equal to 2.495 Å.

The shift of Cd^{2+} cations from their ideal positions can lead to a shortening of some Cd^{2+}-F^- distances to a reasonable value. It results in a distortion of the coordination polyhedra. The displacements are of a statistical nature, because the crystal macrosymmetry remains cubic. They can result in the formation of clusters in the crystal. This problem should be finally solved by the HEED experiments.

One of the possible cluster types corresponding to the shift along the fourfold axis may be postulated using the analogy with other PbF_2 - MF_2 and BaF_2 - MF_2 systems (M = Mg, Zn, Fe, Co, Ni, Mn) [6,16,17]. Compounds with the same stoichiometry (Pb_2MF_6 and Ba_2MF_6) and with tetragonal fluorite-related superstructures are formed in these systems. In the $Pb_{0.67}Cd_{0.33}F_2$ solid solution, the peculiarities of its NMR spectra are explained [18] by the existence of tetragonal ordered domains in the cubic matrix.

Our results are in agreement with the data obtained from the photoemission study of $Pb_{1-x}Cd_xF_2$ solid solutions [19]. According to this work, various Cd-F and Pb-F distances are distributed in a disordered local structure of the solid solution.

4.2. Deficiency of fluoride ions in the lattice position

According to our X-ray diffraction data, the deficient anions are not only shifted from their positions, but they are also spread over the lattice. Local shifts of cations from lattice positions increase the volume available for fluorine ions, thus promoting a fast ionic transport in the nearest neighborhood of the clusters. The deficiency of fluoride ions in lattice positions accounts for their high mobility.

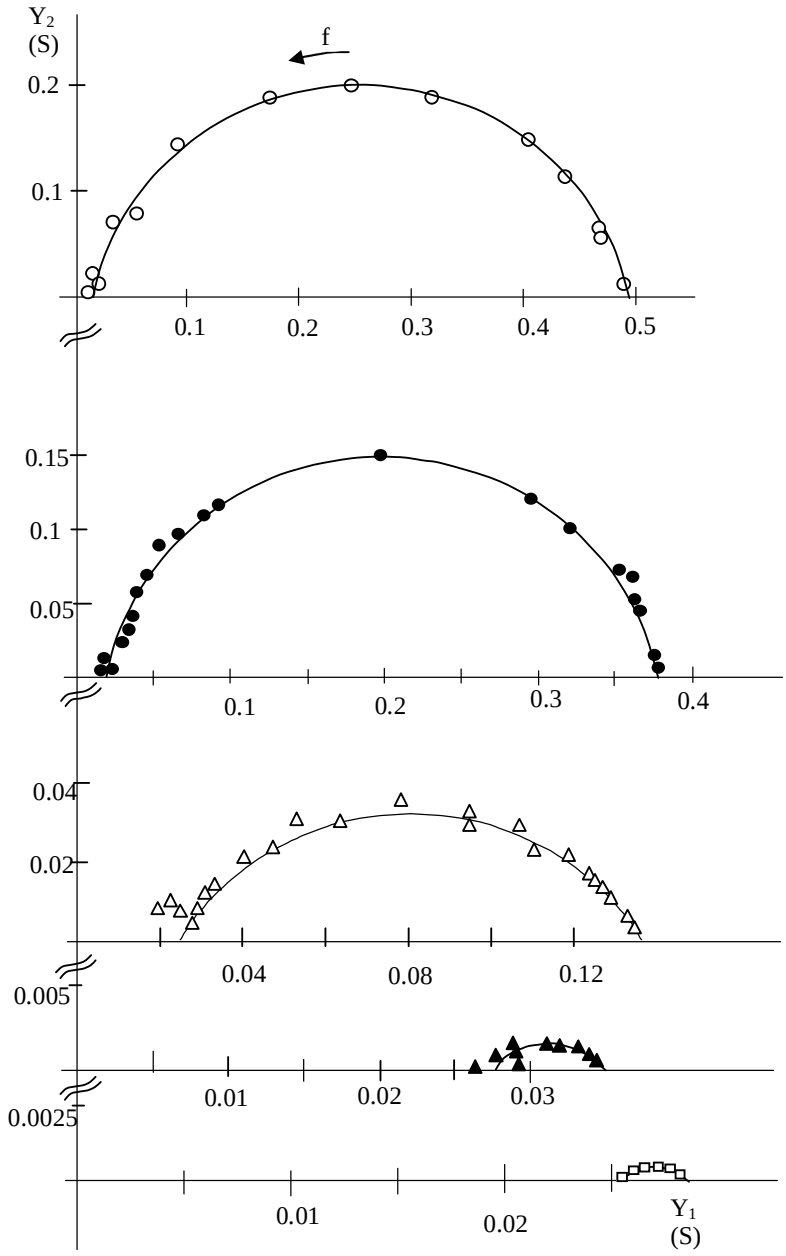

Fig. 4. Admittance diagrams of the $Pb_{0.67}Cd_{0.33}F_2$:1 m/o NaF single crystal at various temperatures (ooo 408 °C, ●●● 323 °C, ΔΔΔ 223 °C, ▲▲▲ 100 °C, □□□ 34 °C).

A similar result was obtained for the high-temperature superionic modification of Li_2SO_4 by using neutron diffraction [20]. In the antifluorite-type structure, cations occupy the tetrahedral *8c* positions (1/4,1/4,1/4), but the experimental population of these positions is only 90 %. 10 % of the cations are spread in a spherical layer surrounding the sulfate group.

We note also a similarity of our results to those of the $Pb_{1-x}Sn_xF_2$ solid solutions (x = 0.1, 0.2) [21]. The high fluoride-ion conductivity of these solutions also results from a large size difference of two isomorphous cations. In these solid solutions, both an incomplete occupation of the base position of fluoride ions as well as a shift of a part of cations along the threefold axis were observed.

The incomplete occupation of lattice fluoride positions can be interpreted as a formation of anti-Frenkel defects. This is the main type of point defects, which are responsible for the anion transport in the fluorite-type structure [22,23]. However, in our samples, the concentration of point defects is so high that it is comparable with their concentration in the superionic states of individual

difluorides, above their diffuse phase transitions [24,25]. This extremely high concentration of anion vacancies and interstitial fluoride ions accounts for the high anionic conductivity of the crystal.

It is interesting that doping with monovalent cations (Li^+, Na^+) has only a small influence on the ionic conductivity of the $Pb_{0.67}Cd_{0.33}F_2$ crystal [9]. Doping with trivalent cations (Ce^{3+}) does not influence the conductivity at all [5]. It seems that the $Pb_{0.67}Cd_{0.33}F_2$ crystal is fully "saturated" with defects and charge carriers, therefore the heterovalent doping (with 1 - 4 m/o MF or RF_3) cannot substantially influence their concentrations.

4.3 Ionic conductivity

The relation between the ionic conductivity, σ_{dc}, and structural data is generally given by the equation

$$\sigma_{dc}(T) = e \cdot N(T) \cdot \mu(T), \tag{5}$$

where e is the charge, N is the concentration, and μ is the mobility of charge carriers.

In our calculations, we suppose that all the fluoride ions, the position of which cannot be localized using X-ray diffraction, are mobile. As the occupation factor of the anionic lattice positions is equal to 0.75, we obtain two vacancies and two mobile interstitial fluoride ions per unit cell. Then we can determine the concentration of charge carriers, $N = 1.05 \times 10^{28}$ m^{-3} (as calculated from the measured unit-cell parameter). Supposing that this concentration is temperature independent, we can, very roughly, estimate the mobility and the jump frequency of mobile fluoride ions, using equation (5).

Due to a large complexity of the system and no information on clustering of defects or migration paths of mobile defects, we had to neglect several important factors (correlation effects, entropy factors, defect-defect interaction, cluster formation etc). However also under these simplifying conditions, our results are in rather good agreement with the data obtained by other techniques [24,25].

Substituting $e = 1.6 \times 10^{-19}$ C, $N = 1.05 \times 10^{28}$ m^{-3}, and the experimental value of the ionic conductivity at 300 K, $\sigma_{dc}(300) = 3.5 \times 10^{-2}$ S m^{-1}, into equation (5), we obtain the value of the mobility of fluoride ions at 300 K ($\mu(300)$) equal to 2.1×10^{-11} m^2/Vs.

Neglecting the entropy term, the hopping model leads to the equation

$$\mu = e \cdot \gamma \cdot a_h^2 \cdot (\nu_0/kT) \cdot \exp(-\Delta H_\mu/kT), \tag{6}$$

where a_h is the hopping distance, γ is the geometrical factor, ν_0 is the attempt-to-jump frequency, and ΔH_μ is the activation enthalpy of the motion.

We could not discern definitely the vacancy and interstitial transport mechanisms because both doping with trivalent cations and doping with monovalent cations did not significantly influence the ionic conductivity. A slight decrease of the conductivity upon a monovalent doping indicates that an interstitial mechanism of the fluoride ion motion is more probable. Therefore, we assume that the interstitialcy mechanism of the fluoride ion transport is dominant. Then, in the fluorite structure we obtain $a_h = a\sqrt{2}/2$ (a is the lattice parameter). As we have no information on the geometry of fluoride jumps we take the value of the geometrical factor, γ, equal to 1. Upon substituting these values and the value of $\mu(300)$ into equation (6), and taking the value of ΔH_μ equal to the conduction activation enthalpy, we can estimate the value of the fluoride ion jump frequency at room temperature, $\nu_i(300) = 3.4 \times 10^6$ s^{-1}. From the temperature dependence of the ionic conductivity (equation (3)), using equations (5) and (6), the temperature dependence of the jump frequency of fluoride interstitials, ν_i, is given by the equation

$$\nu_i = 3.7 \times 10^{12} \exp[-0.359/kT] \ (s^{-1}) \tag{7}$$

The conduction activation enthalpy (0.359 eV) of the $Pb_{0.67}Cd_{0.33}F_2$ crystals is close to that of our nominally pure cubic PbF_2 crystals at temperatures up to 450 K (0.392(5) eV). However, due to a high concentration of defects, the conductivity of the $Pb_{0.67}Cd_{0.33}F_2$ crystals is higher by three orders of magnitude than that of the nominally pure cubic PbF_2 (Fig. 3). We have found also a close value of conduction activation enthalpy ($\Delta H_\sigma = 0.388(2)$ eV) for our best fluoride ion conductor, PbF_2:7 mole % ScF_3. The value of the ionic conductivity of the PbF_2:7 mole % ScF_3 single crystal at 500 K is also very close to that of the $Pb_{0.67}Cd_{0.33}F_2$ single crystal. In the case of the PbF_2:7 mole % ScF_3 crystal, we have clearly proved an interstitialcy transport mechanism [9]. It indicates, but does not prove, an interstitialcy transport mechanism in the $Pb_{0.67}Cd_{0.33}F_2$ crystals, too. Due to defect-defect interaction, a high

concentration of defects in $Pb_{0.67}Cd_{0.33}F_2$ crystals brings about a decrease of the migration enthalpy and of the conduction activation enthalpy.

Our estimations do not take into account the interaction of defects, the migration entropy, and a distribution in jump lengths, jump frequencies, and migration enthalpies. The exact value of γ is unknown for the interstitialcy mechanism in a heavily disordered $Pb_{0.67}Cd_{0.33}F_2$ crystal. However, the calculated value of the pre-exponential factor, ν_o, in the equation (7), agrees reasonably with the frequency observed in infrared studies ($\sim 3 \times 10^{12}$ s^{-1}). This frequency agrees well also with the NMR F19 data [2], according to which the spectrum is represented by a narrow diffusion line even at room temperature.

Acknowledgements

The work was supported by the Russian Foundation for Basic Research, project no. 95-03-09102a, by the Scientific Grant Agency VEGA, Slovak Republic, projects no. 1/8309/01 and 1/9097/02. The authors thank Dr. O. Greis, Technical University Hamburg - Harburg, for his critical reading of the manuscript.

References

[1] I. V. Murin, S. V. Chernov, Izv. Akad. Nauk SSSR, Neorg. Mater. **18**, 168 (1982).
[2] V. A. Vopilov, E. A. Vopilov, V. N. Voronov, V. M. Buznik, Nuclear Magnetic Relaxation and Dynamics of Spin Systems, L.V.Kirenskii, Institute of Physics, Siberian Branch of Academy of Sciences of USSR, Krasnojarsk, 1984, p. 105.
[3] I. Kosacki, Solid State Ionics **28-30**, 449 (1988).
[4] A. de Kozak, M. Samouel, A. Chretien, Rev. Chim. Miner. **8**, 805 (1971).
[5] N. I. Sorokin, I. I. Buchinskaya, B. P. Sobolev, Zh. Neorgan. Khim. **37,** 2653 (1992).
[6] M. Samouel, Rev. Chim. Miner. **8**, 537 (1971).
[7] I. I. Buchinskaya, P. P. Fedorov, B. P. Sobolev, SPIE Proc. **3178**, 59 (1996).
[8] J.-M. Reau, J. Grannec, Inorganic Solid Fluorides, P. Hagenmuller (Ed.), Academic Press, Orlando, p.423, 1985.
[9] V. Trnovcová, P. P. Fedorov, I. I. Buchinskaya, V. Šmatko, F. Hanic, Solid State Ionics **119,** 181 (1999).
[10] I. I. Buchinskaya, P. P. Fedorov, N. I. Sorokin, M. S. Akchurin, B. P. Sobolev, Zh. Neorg. Khim. **41**, 172 (1996).
[11] N. I. Sorokin – private communication.
[12] T. T. Netshisaulu, C. R. A. Catlow, A. V. Chadwick, G. N. Greaves, P. E. Ngoepe, Radiation Effects and Defects in Solids **137**, 159 (1985).
[13] M. A. P. Silva, Y. Messaddeq, V. Briois, M. Poulain, F. Villain, S. J. L. Ribeiro, Solid State Ionics **147**, 135 (2002).
[14] M. Zhiharnovskii, E. G. Ippolitov, Izv. Akad. Nauk SSSR, Neorg. Mater. **5**, 1558 (1969).
[15] I. I. Buchinskaya, P. P. Fedorov, Zh. Neorgan. Khim. **43**, 1202 (1998).
[16] P. P. Fedorov, I. I. Buchinskaya, O. S. Bondareva, G. A. Lovetskaya, M. D. Val'kovskii, Zh. Neorgan. Khim. **40**, 1380 (1995).
[17] D. Babel, A. Tressaud, Inorganic Solid Fluorides, P. Hagenmuller (Ed.), Academic Press, Orlando, p.77, 1985.
[18] A. N. Matsulev, Yu. N. Ivanov, A. I. Livshits, V. M. Buznik, P. P. Fedorov, I. I. Buchinskaya, B. P. Sobolev, Zh. Neorgan. Khim. **45,** 296 (2000).
[19] B. A. Orlowski, B. J. Kowalski, V. Chab, Physica Scripta **35**, 547 (1987).
[20] R. Kaber, L. Nilsson, N. H. Andersen, A. Lunden, J. O. Thomas, J. Phys.: Condens. Matter. **4,** 1925 (1992).
[21] A. B. Lidiard, Crystals with the fluorite structure, W. Hayes (Ed.), Clarendon Press, Oxford, p. 101, 1974.
[22] M. A. Bredig, Colloq. inter. CNRS, No. 5, 183 (1972).
[23] C. R. A. Catlow, J. D. Comins, F. A. Germano, R. T. Harley, W. Hayes, J. Phys. **C 11,** 3197 (1978).
[24] S. Palchoudhuri, G. K. Bichile, Solid State Commun. **67,** 553 (1988).
[25] Y. Ito, T. Mukoyama, K. Ashio, K. Yamamoto, Y. Suga, S. Yoshikado, Ch. Julien, T. Tanaka, Solid State Ionics **106**, 291 (1998).